Dalton Transactions

Fluorescent Mixed Ligand Copper(II) Complexes of Anthracene-appended Schiff Bases: Studies on DNA Binding, Nuclease Activity and Cytotoxicity

Journal:	*Dalton Transactions*
Manuscript ID:	DT-ART-03-2015-000899.R2
Article Type:	Paper
Date Submitted by the Author:	11-May-2015
Complete List of Authors:	Palaniandavar, Mallayan; Bharathidasan University, Chemistry; Central University of Tamil Nadu, Chemistry Jaividhya, Paramasivam; Bharathidasan University, Ganeshpandian, Mani; Bharathidasan University, R, Dhivya; Bharathidasan University, M. A., Akbarsha; Bharathidasan University, Mahatma Gandhi-Doerenkamp Centre (MGDC) for Alternatives to Use of Animals in Life Science Education

Communicated to : Dalton Trans
MS Type : Article
MS ID : DT-ART-03-2015-000899 R2

Fluorescent Mixed Ligand Copper(II) Complexes of Anthracene-appended Schiff Bases: Studies on DNA Binding, Nuclease Activity and Cytotoxicity

Paramasivam Jaividhya,[a] Mani Ganeshpandian,[a] Rajkumar Dhivya,[c] Mohammad Abdulkadher Akbarsha[d,e] and Mallayan Palaniandavar[a,b]*

[a]*School of Chemistry, Bharathidasan University, Tiruchirappalli 620 024, India*
[b]*Distinguished Visiting Professor, Department of Chemistry, Indian Institute of Technology Bombay, Powai 400 076,Mumbai, India*
[c]*Department of Animal Science, Bharathidasan University, Tiruchirappalli 620 024, India*
[d]*Mahatma Gandhi -Doerenkamp Center for Alternatives to use of Animals in Life Science Education, Bharathidasan University, Tiruchirappalli, 620 024, India*
[e]*Visiting Professor, Department of Food Sciences and Nutrition, King Saud University, Riyadh 11451, Kingdom of Saudi Arabia*

To whom correspondence should be addressed, e-mail: palanim51@yahoo.com and palaniandavarm@gmail.com

Abstract

A series of mixed ligand copper(II) complexes of the type $[Cu(L)(phen)(ACN)](ClO_4)_2$ **1–5**, where L is a bidentate Schiff base ligand (*N*^{1}-(anthracen-10-ylmethylene)-*N*^{2}-methylethane-1,2-diamine (L1), *N*^{1}-(anthracen-10-ylmethylene)-*N*^{2},*N*^{2}-dimethylethane-1,2-diamine (L2), *N*^{1}-(anthracen-10-yl-methylene)-*N*^{2}-ethylethane-1,2-diamine (L3), *N*^{1}-(anthracen-10-ylmethylene)-*N*^{2},*N*^{2}-diethylethane-1,2-diamine (L4) and *N*^{1}-(anthracen-10-ylmethylene)-*N*^{3}-methylpropane-1,3-diamine (L5)) and phen is 1,10-phenanthroline, have been synthesized and characterized by spectral and analytical methods. The X-ray crystal structure of **5** reveals that the coordination geometry around Cu(II) is square pyramidal distorted trigonal bipyramidal (τ, 0.76). The corners of trigonal plane of the geometry are occupied by N2 nitrogen atom of phen, N4 nitrogen atom of L5 and N5 nitrogen of acetonitrile while the N1 nitrogen of phen and N3 nitrogen of L5 occupy the axial positions with N1-Cu1-N3 bond angle of 176.0(3)°. All the complexes display a ligand field band (600 - 705 nm) and three less intense anthracene-based bands (345-395 nm) in solution. The K_b values calculated from absorption spectral titration of the complexes ($\pi \rightarrow \pi^*$, 250-265 nm) with Calf Thymus (CT) DNA vary as **5** > **4** > **3** > **2** > **1**. The fluorescence intensity of the complexes (520-525 nm) decreases upon incremental addition of CT DNA, which reveals the involvement of phen rather than the appended anthracene ring in partial DNA intercalation with DNA base stack. The extent of quenching is in agreement with the DNA binding affinities, and the relative increase in viscosity of DNA upon binding to complexes as well. Thus **5** interacts with DNA more strongly than **4** on account of the stronger involvement in hydrophobic DNA interaction of the anthracenyl moiety, which is facilitated by the propylene ligand backbone with chair conformation. The ability of complexes (100 μM) to cleave DNA (pUC19 DNA) in 5 mM Tris-HCl/50 mM NaCl buffer at pH 7.1 in the absence of a reducing agent or light varies as **5** > **4** > **3** > **2** > **1**, which is in conformity with their DNA binding affinities. Interestingly, cytotoxicity studies on MCF-7 human breast cancer cell line show that the IC_{50} value of **5** is less than that of cisplatin for the same cell line, revealing that it can act as an effective cytotoxic drug in a time-dependent manner.

Introduction

Many platinum based drugs show potential efficacy in treating different types of cancer.[1] However, they encounter severe side effects and possess inherent limitations due possibly to their toxicity, drug resistance and covalent mode of their interaction with DNA.[2,3] So, there is considerable attention focused on the design of new metal-based anticancer drugs that involve non-covalent modes of interaction with DNA.[4,5] In this regard, much of the interest is focused on copper(II) complexes as they demonstrate better anticancer activity and show cancer inhibiting activity.[6] The design of new copper(II) complexes, which can bind with specificity to DNA and bring about its cleavage, has become important in the development of new antitumor agents.[7] In particular, the development of complexes, which cleave nucleic acids without any external agent under mild conditions, is attracting great interest in the field of artificial metallonucleases.[8-11] Also, many copper(II) complexes are now known to trigger apoptotic cell death as a consequence of DNA damage occurring inside the cell by activating proapoptotic proteins or antiapoptotic proteins, and lead to induction of apoptosis.[8]

In our laboratory, we have found that mixed ligand copper(II) diimine complexes of different primary ligands, which bind and cleave DNA, exhibit prominent cytotoxicity by inducing apoptosis.[11-16] Very recently, we have reported that certain mixed ligand μ-phenoxo-bridged dinuclear copper(II) complexes with diimine co-ligands exhibit efficient chemical nuclease and protease activities and cytotoxicity.[17] Also, we have found that copper(II) complexes of phenolate and 3N ligands, which bind with DNA by covalent mode of interaction, are non-toxic to normal cells.[18] Further, we have shown that mixed ligand Cu(II) complexes involved in non-covalent DNA interaction display cytotoxicity against human HBL-100 breast cancer lines higher than their corresponding 1:1 metal:ligand complexes covalently bound to DNA as well as cisplatin.[19] We have focused our attention also on non-covalent DNA interactions of various Ru(II),[20] Ni(II),[21] Co(II) [21] and Fe(II)[22] complexes. We have studied the hydrogen bonding potential of the primary ligand on DNA and protein binding by the mixed ligand copper(II) complexes with 2,9-dimethyl-1,10-phenanthroline co-ligand and correlated their DNA binding affinity with anticancer activity.[23]

In this work we have isolated five fluorescent mixed ligand copper(II) complexes $[Cu(L1)(phen)(ACN)](ClO_4)_2$ (**1**), $[Cu(L2)(phen)(ACN)](ClO_4)_2$ (**2**), $[Cu(L3)(phen)$-$(ACN)](ClO_4)_2$ (**3**), $[Cu(L4)(phen)(ACN)](ClO_4)_2$ (**4**) and $[Cu(L5)(phen)(ACN)](ClO_4)_2$ (**5**),

where phen is 1,10-phenanthroline and L is a bidentate Schiff base ligand derived from condensation of 9-anthraldehyde with *N*'-methylethane-1,2-diamine (L1), *N*'-dimethylethane-1,2-diamine (L2), *N*'-ethylethane-1,2-diamine (L3), *N*'-diethylethane-1,2-diamine (L4) and *N*'-methylpropane-1,2-diamine (L5) (**Scheme 1).**

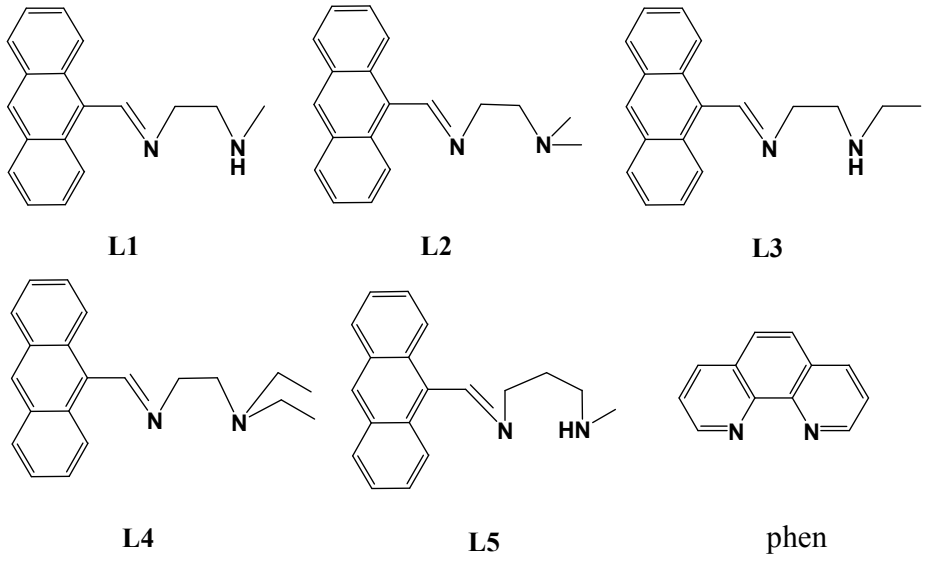

Scheme 1: Structure of primary and co-ligands

As DNA is the primary pharmacological target of many antitumor compounds, the study of interaction of **1**–**5** with calf thymus DNA (CT DNA) is of paramount importance in understanding the mechanism of tumor inhibition. The propensity and mode of DNA binding of the complexes has been probed by using absorption spectral titration. The anthracenyl ligand moiety is expected to partially intercalate into DNA with extended π-electron systems enhancing the DNA binding affinity and hence cytotoxicity of the complexes.[24] The anthracene-based compound pseudourea has been tested in clinical trials as an anticancer drug[25a] and several anthracene derivatives are known to have significant biological activities against certain types of cancers.[25] Also, from a photochemical viewpoint, anthracene derivatives are important fluorescent chromophores capable of acting as photo-signaler for charge transfer (CT) complexes, and some fluorescent chemosensors of small biomolecules and metal ions based on anthracene derivatives have been fabricated and widely investigated.[26,27] So, copper complexes with a fluorescent tag like anthracene chromophore may be useful for visualizing them within the cells. This approach has been found to be useful in studying the cellular responses of several

fluorescent copper(II) complexes.[28] Reedijk and his co-workers have reported that [Cu(9-Accm)(phen)Cl], where 9-Accm is 1,7-(di-9-anthracene-1,6-heptadiene-3,5-dione), provides valuable information about cellular processes due to its intrinsic fluorescence.[29] As the present complexes are fluorescent, the interaction of the complexes with DNA has been investigated using emission spectral titration also. The phen co-ligand has been chosen as it may be involved in partial intercalation with DNA base pairs and enhance the DNA binding affinity, and the liphophilic phen moiety has been shown to facilitate the passage of complexes through cell membrane.[30, 31] Interestingly, the complexes are found to partially intercalate into DNA through the partial insertion of phen co-ligand rather than the anthracenyl ligand moiety. The DNA cleavage properties and cytotoxicity of the complexes have been also investigated. We have found that **5**, which shows stronger DNA binding affinity and more efficient cleavage of plasmid DNA than other complexes, exhibits higher cytotoxicity against human breast cancer (MCF-7) cell lines with its potency being higher than that of cisplatin.

Experimental

Materials

All reagents and chemicals of analytical grade were purchased from commercial sources and used without further purification. Solvents were purified by standard procedures.[32] *N*'-Methylethane-1,2-diamine, *N*'-dimethylethane-1,2-diamine, *N*'-ethylethane-1,2-diamine, *N*'-diethylethane-1,2-diamine and *N*'-methylpropane-1,2-diamine were purchased from Aldrich. Copper(II) perchlorate hexahydrate and 1,10-phenanthroline were purchased from Merck. Calf thymus DNA and ethidium bromide were from Sigma. The supercoiled pUC19 DNA (cesium chloride purified) and agarose (molecular biology grade) were purchased from Bangalore Genei (India). Tris–HCl buffer solution of pH 7.1 was prepared using deionized, sonicated and triply distilled water. All the five ligands L1–L5 were synthesized using known procedures,[33] which involve the reaction of 9-anthraldehyde with the corresponding amine to form Schiff bases.

Experimental Methods

Microanalyses (C, H and N) were carried out with a Vario EL elemental analyzer. UV-Vis spectra were recorded on a Shimadzu 2450 UV-Vis spectrophotometer using cuvettes of 1 cm path length. ^{1}H NMR spectra were recorded on a Bruker 400 MHz NMR spectrometer. Mass

spectrometry was performed on a QTOF ESI-MS spectrometer using acetonitrile (ACN) solvent. Emission intensity measurements were carried out by using a Jasco F 6500 spectrofluorimeter. The viscosity measurements were carried out on a Schott Gerate AVS 310 automated viscometer thermostated at 25 ^{o}C in a constant temperature bath.

Solutions of DNA in the buffer 50 mM NaCl/5 mM Tris HCl buffer (pH = 7.1) in water gave the ratio of UV absorbance at 260 and 280 nm, A_{260}/A_{280}, of 1.9,[34] indicating that the DNA was sufficiently free of protein. Concentrated stock solutions of DNA were prepared in a 50 mM NaCl/5 mM Tris HCl buffer and sonicated for 25 cycles, where each cycle consisted of 30 s with 1 min intervals. The concentration of DNA in nucleotide phosphate (NP) was determined by UV absorbance at 260 nm after 1:100 dilutions by taking the extinction coefficient ε_{260} as 6600 M^{-1} cm^{-1}. Stock solutions of DNA were stored at 4 ^{o}C and used after no more than 4 days. Supercoiled plasmid pUC19 DNA was stored at -20 $^{\circ}$C and the concentration of DNA in base pairs were determined by UV absorbance at 260 nm after appropriate dilutions taking ε_{260} as 13100 $M^{-1}cm^{-1}$. Concentrated stock solutions of copper complexes were prepared by dissolving calculated amounts of copper complexes in required amounts of acetonitrile:water mixed solvent (1:10 v/v) and diluted suitably with the corresponding buffer to required concentrations for all experiments. The ability of **1 - 5** to cleave DNA was examined by following the conversion of supercoiled plasmid DNA to open circular DNA or linear DNA using agarose gel electrophoresis to separate the cleavage products.

Synthesis of ligands

Synthesis of N^1-(anthracen-10-ylmethylene)-N^2-methylethane-1,2-diamine, L1

N'-methylethane-1,2-diamine (0.74 g, 10 mmol) in methanol (20 mL) was added dropwise to 9-anthraldehyde (2.06 g, 10 mmol) in methanol (20 mL). The mixture was stirred overnight to get N^1-(anthracen-10-ylmethylene)-N^2-methylethane-1,2-diamine as a bright yellow solid. The yield was 2.09 g (80%). ^{1}H NMR (400 MHz, $CDCl_3$): 2.07 (s, -NH), 2.49 (d, CH_3) 3.67 (t, CH_2), 2.94 (t, CH_2), 7.35 – 7.89 (m, 9H).

Synthesis of N^1-(anthracen-10-ylmethylene)-N^2,N^2-dimethylethane-1,2-diamine, L2

The ligand L2 was prepared by the method adopted for the preparation of L1, except that *N*'-dimethylethane-1,2-diamine (0.88 g, 10 mmol) was used instead of *N*'-methylethane-1,2-

diamine. Yield: 2.07 g (75%). ^{1}H NMR (400 MHz, $CDCl_3$): 2.29 (s, -N(CH_3)$_2$) 8.14 (s, -CH=N), 7.36 – 7.87 (m, 9H).

Synthesis of N^1-(anthracen-10-ylmethylene)-N^2-ethylethane-1,2-diamine, L3

The ligand L3 was prepared by the method adopted for the preparation of L1, except that N'-dimethylethane-1,2-diamine (0.88 g, 10 mmol) was used instead of *N*'-methylethane-1,2-diamine. Yield: 2.2 g (80%). ^{1}H NMR (400 MHz, $CDCl_3$): 2.07 (m, -NH), 2.57 (m, -N-CH_2), 7.34 – 7.89 (m, 9H).

Synthesis of N^1-(anthracen-10-ylmethylene)-N^2,N^2-diethylethane-1,2-diamine, L4

The ligand L4 was prepared by the method adopted for the preparation of L1, except that *N*'-diethylethane-1,2-diamine (1.16 g, 10 mmol) was used instead of *N*'-methylethane-1,2-diamine. Yield: 2.43 g (84%). ^{1}H NMR (400 MHz, $CDCl_3$): 2.41 (m, -N-CH_2), 1.07 (m, CH_3), 3.01 (t, CH_2), 7.34 – 7.92 (m, 9H).

Synthesis of N^1-(anthracen-10-ylmethylene)-N^3-methylpropane-1,3-diamine, L5

The ligand L5 was prepared by the method adopted for the preparation of L1, except that *N*'-methylpropane-1,2-diamine (0.88 g, 10 mmol) was used instead of *N*'-methylethane-1,2-diamine. Yield: 2.32 g (80%). 1H NMR (400 MHz, $CDCl_3$): d 2.04 (m, -NH), 2.43 (s, -NCH_3), 7.31 – 7.91 (m, 9H).

Preparation of Copper(II) complexes

Caution!

Perchlorate salts of metal complexes with organic ligands are potentially explosive. Although no difficulty was encountered during the synthesis, they should be prepared in small quantities and handled with great care.

Preparation of [Cu(L1)(phen)(ACN)](ClO_4)$_2$ (1)

The complex **1** was prepared by addition of a methanolic solution (10 mL) of a mixture of 1,10-phenanthroline (0.18 g, 1 mmol) and N^1-(anthracen-10-ylmethylene)-N^2-methylethane-1,2-diamine (0.26 g, 1 mmol) to a solution of copper(II) perchlorate hexahydrate (0.37 g, 1 mmol) in

methanol (15 mL) and then stirring at 40 °C for 2 h. The green solid obtained was collected by suction filtration, washed with small amounts of cold methanol and diethyl ether and then dried in vacuum. It was then recrystallized from aqueous acetonitrile. Anal. Calcd for $C_{32}H_{29}Cl_2CuN_5O_8$: C, 51.52; H, 3.92; N, 9.39%. Found: 51.59, H, 3.93, N, 9.34%. Mol. Wt.: 746.05. ESI-MS: $[Cu(L1)(phen)(ACN)]^{2+}$ displays a peak at *m/z* 273.17 (calcd 273.08). Yield: 0.63 g (85%).

Preparation of [Cu(L2)(phen)(ACN)](ClO$_4$)$_2$ (2)

This complex was prepared by adopting the procedure used for the isolation of **1** but by using N^1-(anthracen-10-ylmethylene)-N^2,N^2-dimethylethane-1,2-diamine instead of N^1-(anthracen-10-ylmethylene)-N^2-methylethane-1,2-diamine. The dark green solid obtained was collected by suction filtration, washed with small amounts of cold methanol and diethyl ether and then dried in vacuum. It was recrystallized from aqueous acetonitrile. Anal. Calcd for $C_{33}H_{31}Cl_2CuN_5O_8$: C, 52.15; H, 4.11; N, 9.21%. Found: C, 52.19; H, 4.13; N, 9.24%. Mol. Wt.: 760.08. ESI-MS: $[Cu(L2)(phen)]^{2+}$ displays a peak at *m/z* 259.69 (calcd 259.58). Yield: 0.62 g (82%).

Preparation of [Cu(L3)(phen)(ACN)](ClO$_4$)$_2$ (3)

This complex was prepared by adopting the procedure used for the isolation of **1** but by using N^1-(anthracen-10-ylmethylene)-N^2-ethylethane-1,2-diamine instead of N^1-(anthracen-10-ylmethylene)-N^2-methylethane-1,2-diamine. The dark green solid obtained was collected by suction filtration, washed with small amounts of cold methanol and diethyl ether and then dried in vacuum. It was recrystallized from aqueous acetonitrile. Anal. Calcd for $C_{33}H_{31}Cl_2CuN_5O_8$: C, 52.15; H, 4.11; N, 9.21%. Found: C, 52.19; H, 4.12; N, 9.26%. Mol. Wt.: 760.08. ESI-MS: $[Cu(L3)(phen)]^{2+}$ displays a peak at *m/z* 259.78 (calcd 259.58). Yield: 0.59 g (82%).

Preparation of [Cu(L4)(phen)(ACN)](ClO$_4$)$_2$ (4)

This complex was prepared by adopting the procedure used for the isolation of **1** but by using N^1-(anthracen-10-ylmethylene)-N^2,N^2-diethylethane-1,2-diamine instead of N^1-(anthracen-10-ylmethylene)-N^2-methylethane-1,2-diamine. The dark green solid obtained was collected by suction filtration, washed with small amounts of cold methanol and diethyl ether and then dried in vacuum. It was then recrystallized from aqueous acetonitrile. Anal. Calcd for

$C_{35}H_{35}Cl_2CuN_5O_8$: C, 53.34; H, 4.48; N, 8.89%. Found: C, 53.38; H, 4.41; N, 8.82%. Mol. Wt.: 788.13. ESI-MS: $[Cu(L4)(phen)(ACN)]^{2+}$ displays a peak at *m/z* 294.77 (calcd 294.11). Yield: 0.62 g (79%)

Preparation of $[Cu(L5)(phen)(ACN)](ClO_4)_2$ (5)

This complex was prepared by adopting the procedure used for the isolation of **1** but by using N^1-(anthracen-10-ylmethylene)-N^3-methylpropane-1,3-diamine instead of N^1-(anthracen-10-ylmethylene)-N^2-methylethane-1,2-diamine. The dark green crystalline solid obtained was collected by suction filtration, washed with small amounts of cold methanol and diethyl ether and then dried in vacuum. Green colored crystals of **5** suitable for X-ray diffraction studies were obtained by dissolving the complex in aqueous acetonitrile and allowing it for crystallization. Anal. Calcd for $C_{33}H_{31}Cl_2CuN_5O_8$: C, 52.15; H, 4.11; N, 9.21%. Found: C, 52.13; H, 4.16; N, 9.25%. Mol. Wt.: 760.08. ESI-MS: $[Cu(L5)(phen)(ACN)]^{2+}$ displays a peak at *m/z* 280.12 (calcd 280.09).Yield: 0.64 g (85%).

X-Ray Crystallography

The crystal **5** of suitable size selected from the mother liquor was mounted on the tip of a glass fiber and cemented using epoxy resin. Intensity data for the crystals were collected using MoKα (λ = 0.71073 Å) radiation on a Bruker SMART APEX diffractometer equipped with a CCD area detector at 100 and 293 K. The SMART[35] program was used for collecting frames of data, indexing the reflections, and determining the lattice parameters. SAINT[35] program for integration of the intensity of reflections and scaling; and the SHELXTL[36] program for space group and structure determination, and least-squares refinements on F^2. The structure was solved by heavy atom method and other non-hydrogen atoms were located in successive difference Fourier syntheses. Crystal data and additional details of the data collection and refinement of the structure are presented in **Table 1**. The selected bond lengths and angles are listed in **Table 2**.

DNA Binding Experiments

Concentrated stock solutions of metal complexes were prepared by dissolving them in acetonitrile:water mixed solvent (1:10 v/v) and diluting them with 50 mM NaCl/5 mM Tris HCl buffer solution at pH 7.1 buffer to required concentrations for all the experiments. For absorption

and emission spectral experiments the DNA solutions were pretreated with solutions of metal complexes to ensure no change in the metal complex concentrations. Absorption spectral titration experiments were performed by maintaining a constant concentration of the complex and varying the nucleic acid concentration. This was achieved by dissolving an appropriate amount of the metal complex and DNA stock solutions while maintaining the total volume constant (1 mL). This results in a series of solutions with varying concentrations of DNA but with a constant concentration of the complex. The absorbance (A) was recorded after successive additions of CT DNA.

Emission intensity measurements were carried out using JASCO F 6500 spectrofluorimeter. 5 mM Tris-HCl/50 mM NaCl buffer solution was used as a blank to make preliminary adjustments. The excitation wavelength was fixed and the emission range was adjusted before measurements. The metal complexes were then added to calf thymus DNA and their effect on the emission intensity was measured. Fixed amounts (1×10^{-5} M) of complexes were titrated with increasing amounts of CT DNA, over a range of DNA concentrations from 5 to 100 μM. Excitation wavelengths of the samples were about 380-385 nm, scan speed was 480 nm/min, and both of excitation and emission slit widths were 10 nm. All experiments were conducted at a constant room temperature in Tris-HCl buffer solution. The fluorescence quenching experiments were carried out by the similar operation as absorbance titrations. The steady-state luminescence titration data have been analyzed using Mc Ghee von Hippel equation[37] for non-co-operative binding model by non-linear least-squares analysis. A known amount (10 μM) of **1** – **5** were titrated with DNA over a range of the DNA concentration (5×10^{-6} to 1×10^{-4} M, R = 0 – 10 = [DNA]/[Cu(II) complex]). The concentration of the bound Cu(II) complex was calculated using equation (1):

$$c_b = c[(I–I_0)/(I_{max}–I_0)] \qquad (1)$$

where c is the total Cu(II) complex concentration, I and I_0 are the emission intensities in the presence and absence of DNA, and I_{max} is the fluorescence of the totally bound complex. The concentration of the free complex, c_f, is equal to $(c - c_b)$. A plot of r/c_f vs r, where r is c_b/[DNA], was constructed according to the McGhee and von Hippel equation (2):

$$2r/c_f = K_b(1 - 2nr)[(1 - 2nr)/\{1 - 2(n - 1)r\}]^{n-1} \qquad (2)$$

where K_b represents the intrinsic binding constant of the complexes with DNA and n is the size of a binding site in base pairs.

For viscosity measurements, CT DNA concentration was kept constant (500 μM in NP) and the concentration of metal complexes varied ($1/R$ = [Cu]/[DNA] = 0.0 – 0.50). The flow times were noted from the digital timer attached with the viscometer. Data are presented as η/η_0 *vs.* $1/R$, where η is the relative viscosity of DNA in the presence of the copper(II) complex and η_0 is the relative viscosity of DNA alone. Relative viscosity values were calculated from the observed flow time of the DNA solution (t) corrected for the flow time of the buffer alone (t_0), using the expression $\eta_0 = (t - t_0)/t_0$.

DNA Cleavage Experiments

DNA cleavage experiments were carried out as described previously.[19,38]

Cell Culture

The MCF 7 human breast cancer cell lines were obtained from National Center for Cell Science (NCCS), Pune, India. The cells were cultured in RPMI 1640 medium (Biochrom AG, Berlin, Germany), supplemented with 10% fetal bovine serum (Sigma, USA), cisplatin (Getwell pharmaceuticals, India), mitomycin C (Sigma, USA) and 100 U/mL penicillin and 100 μg/mL streptomycin as antibiotics (Himedia, Mumbai, India), in 96 well culture plates, at 37 °C in a humidified atmosphere of 5% CO_2 in a CO_2 incubator (Heraeus, Hanau, Germany). All experiments were performed using cells from passage 15 or less.

MTT Assay and AO/EB staining assay

MTT (3-(4,5-dimethylthiazol-2-yl)-2,5-diphenyltetrazolium bromide) and AO/EB staining assay were carried out as described previously.[19,23,39] The complexes in the concentration range of 0.05 – 50 μg/mL, dissolved in DMSO (Sigma-Aldrich, St. Louis, MO, USA) were added to the wells 24 h after seeding of 5×10^3 cells per well in 200 μL of fresh culture medium. DMSO was used as the vehicle control. After 24 and 48 h, 20 μL of MTT solution [5 mg/mL in phosphate-buffered saline (PBS)] was added to each well and the plates were wrapped with aluminum foil and incubated for 4 h at 37 °C. The purple formazan product formed was dissolved by addition of 100 μL of 100% DMSO to each well. The absorbance was monitored at

570 nm (measurement) and 630 nm (reference) using a 96 well plate reader (Bio-Rad, Hercules, CA, USA). The stock solutions of the copper complexes were prepared in DMSO and in all the experiments the percentage of DMSO was maintained in the range of 0.1 – 1%. DMSO by itself was found to be non-toxic to the cells till 1% concentration. Data were collected for four replicates each and used to calculate the mean. The percentage inhibition was calculated from these data using the formula:

$$\frac{\text{Mean OD of untreated cells (control) - Mean OD of treated cells}}{\text{Mean OD of untreated cells (control)}} \times 100$$

The IC_{50} values were calculated using *Table Curve 2D*, version 5.01.

Results and Discussions

Syntheses and Characterization of Complexes

The mononuclear mixed ligand copper(II) complexes of the type $[Cu(L)(phen)(ACN)](ClO_4)_2$ (**1** - **5**), where L is a simple bidentate (2N) Schiff base ligand and phen is 1,10-phenanthroline, have been isolated by adding a methanolic solution of one equivalent of copper(II) perchlorate hexahydrate to a mixture of one equivalent each of the ligand (**L1-L5**) and phen in methanol solution. All the complexes have been obtained in good yields and were characterized by elemental analysis, ESI-MS (**Figure S1**) and UV-Vis absorption spectroscopy. The molecular formula $[Cu(L)(phen)(ACN)](ClO_4)_2$ of the complexes is consistent with the X-ray crystal structure of $[Cu(L5)(phen)(ACN)](ClO_4)_2$ **5**. For the present study stock solutions of the complexes were prepared in 5 mM Tris-HCl/50 mM NaCl buffer at pH 7.1 and in acetonitrile:water mixed solvent (1:10 v/v). All the complexes exhibit only one broad band in the visible region (600 – 705 nm) with very low absorptivity (**Table 3**) in 5 mM Tris-HCl/50 mM NaCl buffer at pH 7.1, which is consistent with a square based copper(II) coordination geometry of the complexes. It is possible that on dissolution in acetonitrile the complexes undergo a structural change from trigonal bipyramidal (*cf*. below) to a square based geometry. The intense absorption bands observed in the region 253 - 265 nm are attributed to intra-ligand $\pi \rightarrow \pi^*$ transitions within the coordinated Schiff base and phen ligands while the

less intense absorption bands observed in the region 349 - 391 nm are characteristic of intra-ligand ($\pi \rightarrow \pi^*$) transitions located on the anthracene moiety.[40] The frozen solution EPR spectra of the complexes in ACN solvent are axial with $g_{\|} > g_{\perp} > 2.0$ and $G = [(g_{\|} - 2)/(g_{\perp} - 2)] = 3.7 - 4.6$, which supports the square-based geometry around copper(II) in solution. A square-based CuN_4 chromophore is expected to show a $g_{\|}$ value of 2.200 and $A_{\|}$ value of 200×10^{-4} cm^{-1}, and a distortion from square planar coordination geometry or axial interaction would increase the $g_{\|}$ value and decrease the $A_{\|}$ value.[41] The observed values of $g_{\|}$ (2.197 – 2.191) and $A_{\|}$ (188 – 202 $\times 10^{-4}$ cm^{-1}) for **1** – **5** reveal the presence of a square-based CuN_4 chromophore with no or very weak axial interaction in solution. It is evident that complex **5** with trigonal bipyramidal coordination geometry in the solid state (cf. below) undergoes structural change upon dissolution, as expected. The molar conductivity of **1 - 5** in acetonitrile solution (Λ_M , 212 – 226 Ω cm^2 mol^{-1}) falls in the range[42] for 1:2 electrolytes, which supports the existence of dicationic complex species in solution.

Description of Structure of [Cu(L5)(phen)(ACN)]$(ClO_4)_2$ 5

The single crystal X-ray structure of [Cu(L5)(phen)(ACN)]$(ClO_4)_2$ **5** consists of monomeric units of the complex dication. An ORTEP view of the coordination environment of the complex dication including the atom numbering scheme is shown in **Figure 1** and the selected bond distances and bond angles are listed in **Table 2**. The copper atom of the dication is coordinated by both the nitrogen atoms (N3, N4) of the Schiff base ligand (L5), both the nitrogen atoms (N1, N2) of phen co-ligand and the nitrogen (N5) atom of acetonitrile solvent (ACN). The coordination geometry around copper(II) is best described as square pyramidal distorted trigonal bipyramidal (SPDTBP)[43,44] as evident from the value of the trigonal index[45] τ, 0.76 [$\tau = (\alpha-\beta)/60$, where α = 176.0° and β = 130.3°; τ is 1 for a perfect trigonal bipyramidal geometry and is zero for a perfect square pyramidal geometry]. The corners of trigonal plane of the geometry are occupied by N2 nitrogen of phen (Cu-N2, 2.096(6) Å), N4 nitrogen of L5 (Cu-N4, 2.043(6) Å) and N5 nitrogen of acetonitrile (Cu-N5, 2.201(6) Å) while N1 nitrogen of phen (Cu-N1, 1.996(6) Å) and N3 nitrogen of L5 (Cu-N3, 2.010(6) Å) occupy the axial positions with N1-Cu1-N3 bond angle of 176.0(3)°. The $Cu–N3_{amine}$ bond is expected to be longer than the $Cu–N4_{imine}$ bond due to sp^3 and sp^2 hybridizations of the amine and imine nitrogen atoms respectively; however, it is shorter. The $Cu\text{-}N1_{phen}$ (1.996(6) Å) bond is also shorter than the equatorial $Cu\text{-}N2_{phen}$ (2.096(6)

Å) bond. Thus the N1 nitrogen of phen and N3 nitrogen of L5 occupy the apical positions at distances shorter than the equatorial nitrogen atoms revealing that the coordination geometry corresponds to compressed trigonal bipyramidal. The alkane backbone of ligand L5 possesses a chair conformation expected of a six-membered chelate ring.

DNA Binding Studies

Absorption Spectral Titration

Electronic absorption spectroscopy is an effective method in examining the mode and extent of binding of a metal complex with DNA. Upon adding CT DNA to **1** – **5** (R = [DNA base pairs]/[complex] = 1 – 25) in 5 mM Tris HCl/50 mM NaCl buffer solution, the ligand-based $\pi \rightarrow \pi^*$ spectral band (253 – 265 nm) exhibits a strong decrease in absorption intensity (hypochromism, $\Delta\varepsilon$, 20 – 46%, **Table 4**, **Figure 2**) with a small red-shift (2 – 4 nm) in band position. As the extent of hypochromism is commonly associated with the strength of DNA interaction, the observed order of decrease in hypochromism, **5** > **4** > **3** > **2** > **1**, implies the decrease in DNA binding affinities of complexes in this order (cf. below). Upon partial insertion of coordinated phen co-ligand into DNA base pairs and coupling of the π^* orbital of phen with π orbital of base pairs, the π^* orbitals of phen ring are partially filled with electrons, leading to a decrease in the transition probabilities and hence hypochromism,[46] and the moderate red-shifts observed (2 – 4 nm) supports the partial intercalation of phen. It may be noted that the three less intense absorption bands (349-391 nm) characteristic of intra-ligand ($\pi \rightarrow \pi^*$) transitions located on the anthracene moiety undergo relatively very small decrease in intensity indicating the non-involvement of anthracene ring in partial intercalation with DNA base pairs. Molecular model building studies reveal that the partial DNA intercalation of anthracenyl moiety, which is located above but away from the phen ring on account of rotation around N-CH_2- group, is sterically hindered by the propylene group and *N*-alkyl side chain. On the other hand, interestingly, the anthracenyl moiety appended to the Ru(II)-arene complex [Ru(η^6-arene)(L)Cl]$^+$,[31] where L is anthracene-appended homopiperazine, is involved in strong partial intercalation into DNA base pairs, as revealed by the strong decrease in absorption intensities and red-shifts in the anthracenyl absorption bands. In order to compare the DNA binding affinities quantitatively, the intrinsic binding constant K_b for **1** – **5** bound to CT DNA was obtained by monitoring the

changes in absorbance of the $\pi \rightarrow \pi^*$ spectral band (253 – 265 nm) upon increasing the concentration of DNA by using the equation,[47]

$$[DNA]/(\varepsilon_a-\varepsilon_f) = [DNA]/(\varepsilon_b-\varepsilon_f) + 1/K_b(\varepsilon_b-\varepsilon_f) \quad (3)$$

where [DNA] is the concentration of DNA in base pairs, the apparent absorption coefficient ε_a, ε_f and ε_b corresponds to A_{obs}/[Complex], the extinction coefficient for the free copper complex and the extinction coefficient for the copper complex in the fully bound form, respectively. In the plot of [DNA]/(ε_a-ε_f) versus [DNA], the value of K_b is given by the ratio of slope to intercept. The binding constants determined (K_b, 0.9 – 2.3 × 10^5 M^{-1}) varies in the order: **5** > **4** > **3** ≥ **2** > **1**, which is the same as that for the hypochromism (cf. above). They are lower than those observed for the typical classical intercalator ethidium bromide (EthBr) (K_b, 4.94 × 10^5 M^{-1} in 25 mM Tris-HCl/40 mM NaCl buffer, pH 7.9),[48] suggesting that the coordinated phen ring is only partially inserted into the DNA base pairs. The DNA binding affinities of **1** – **5** are much higher than that of the neutral complex [Cu(imda)(phen)] (K_b, 0.6 × 10^3 M^{-1})[49] and higher than those of the dicationic complexes, $[Cu(pmdt)(phen)]^{2+}$ (K_b, 3.1 × 10^3 M^{-1})[13] and $[Cu(dipica)(phen)]^{2+}$ (K_b, 4.0 × 10^3 M^{-1}),[50] but are of the order similar to that of the dicationic complex $[Cu(bba)(phen)]^{2+}$ (K_b, 0.3 × 10^5 M^{-1}),[12] obviously because of the strong hydrophobic interaction of the anthracenyl moiety, as modulated by the propylene/ethylene and *N*-alkyl side chain groups, and the benzimidazolyl ligand moiety (bba) with DNA. It has been found that the order of K_b values (3.8-4.8 × 10^5 M^{-1}) observed for certain complexes with appended anthracenyl moiety is of the same order as the present complexes.[24,40] Also, the propylene backbone of L5 ligand (**5**) with chair conformation facilitates strong hydrophobic interaction of anthracenyl moiety with DNA higher than the ethylene backbone of L4 (**4**) leading to the higher DNA binding affinity of the former. Further, the two ethyl groups on the amine nitrogen of the primary ligand in **4** are involved in hydrophobic DNA interaction stronger than the only one ethyl group in **3** leading to the higher DNA binding affinity of **4**. Similarly, the DNA binding affinity of **2** with two methyl groups is higher than that of **1** with only one methyl group. Also, **3** with one ethyl group shows the same DNA binding affinity as **2** with two methyl groups, and **4** with two ethyl groups shows DNA binding affinity higher than **2** with two methyl groups. Thus, the hydrophobic interaction

of anthracenyl ring, as modulated by propylene/ethylene ligand backbone, and of the methyl/ethyl side chain of the primary ligand with DNA dictates the DNA binding affinity of the mixed ligand complexes.

Emission Spectral studies

The fluorescence emission intensity of **1**–**5** (λ_{em}, 520-525 nm; λ_{ex}, 380-385 nm) decreases upon adding CT DNA (**Figure 3A**), without any change in position of the emission maximum, and the extent of quenching increases with increase in DNA concentration. The involvement of anthracenyl ring in partial intercalation with DNA base pairs would be expected to lead to stabilization of the excited state and hence enhance the emission intensity. So the present observation of decrease in emission intensity supports the non-involvement of anthracenyl ring in partial DNA intercalation and reveals that changes in the average local environment of the anthracenyl chromophore of the complexes upon DNA binding is dictated by the ethylene/propylene ligand backbone and the *N*-alkyl side chains on the primary ligand. The binding data were fitted (**Figure 3B**) using equation (2), and the observed intrinsic binding constants are collected in **Table 5** (K_b', 0.6 – 13.0 × 10^5 M^{-1}) along with the DNA binding site sizes (*n*, 3.0 – 7.2 base pairs). Though determined by a different principle, K_b' has the same significance as K_b from UV-Vis spectral titration and a plot of K_b vs K_b' is linear (**Figure 4**), supporting the effect of hydrophobicity of the primary ligands in tuning the DNA binding affinity (cf. above). Thus the propylene backbone of L5 ligand (**5**) with chair conformation rather than the ethylene backbone in **1** - **4** facilitates stronger hydrophobic interaction of anthracenyl moiety with DNA leading to confer a higher DNA binding affinity on **5**.

Viscosity Measurements

Hydrodynamic measurements that are sensitive to changes in length are regarded as the most important test to provide reliable evidence for DNA binding modes in solution.[11-13] The values of relative viscosity (η/η_0), where η and η_0 are the specific viscosities of DNA in the presence and absence of the complexes, were determined for **1** – **5** and plotted against values of 1/R = 0.0 – 0.5 (R = [DNA base pairs]/[complex]) (**Figure 5**). The viscosity steadily increases upon increasing the amount of complex added to CT DNA. The ability of complexes to increase the viscosity of DNA is lower than that of the classical intercalator EthBr as expected and varies as **5** > **4** > **3** > **2** > **1**, which is consistent with the trends in DNA binding affinities as determined by

absorption and emission spectral studies. Thus the partial intercalation of extended aromatic ring of phen, supported by the hydrophobic interaction of anthracenyl moiety, as modulated by the propylene/ethylene ligand backbone, and the alkyl side chain on the primary ligand, lead to higher elongation of the DNA double strand, and hence higher enhancement in viscosity of CT DNA.

DNA Cleavage Studies

The ability of **1** - **5** to cleave DNA was assayed with the aid of gel electrophoresis on supercoiled (SC) pUC19 plasmid DNA as the substrate in a medium of 5 mM Tris-HCl/50 mM NaCl buffer (pH 7.1) in the absence of external additives. Upon incubation of the plasmid DNA with **1** - **5** (100 μM) for 1h at 37 °C followed by electrophoresis, the fastest migration is observed for the SC form (form I). Upon cleavage a single strand of the SC DNA relaxes to produce a slower-moving nicked circular (NC) form (form II). As no linear form (LC, form III) is discerned between forms I and II, it is evident that both the DNA strands are not cleaved by **1**–**5**. The extent of cleavage of SC form to NC form (**Figure 6**, **Table 6**) follows the order, **5** (99.2%) > **4** (96.1%) > **3** (77.5%) > **2** (76.1 %) > **1** (70.9 %). While **4** and **5** show the highest nuclease activity, **1**, **2** and **3** show moderate nuclease activity, which is consistent with the changes in DNA binding affinity on account of the partial intercalation of phen ring as well as the hydrophobic interaction of appended anthracenyl moiety, as modulated by the ethylene/propylene ligand backbone, and the alkyl side chain of the primary ligand with DNA surface. When the concentrations of **4** and **5** (10-100 μM) are increased by keeping the DNA concentration (40 μM) constant, the amount of SC form decreases whereas that of NC form II increases. Remarkably, **5** causes maximum degradation of DNA at 40 μM complex concentration whereas **4** causes the same percentage of DNA cleavage but at a higher concentration of 100 μM (**Figure 7**, **Table 7**, **8**). This interesting behavior of **5**, which is consistent with its higher DNA binding affinity and elongation of DNA double strand, prompted us to analyze the kinetic aspects of DNA gel electrophoresis data obtained for **5** under the above conditions (**Figure S2**). The decrease in amount of SC form follows pseudo-first-order kinetics and fits well into a single-exponential decay curve (**Figure S2**). Under constant substrate (DNA) concentration and varying catalyst concentration (pseudo Michaelis Menten conditions), we

obtained V_{max} = 0.0262 min^{-1}, K_M = 31.4 μM and k_{cat} = 6.54×10^{-4} (where k_{cat} is defined as V_{max}/[catalyst]) for the DNA cleavage. The rate of DNA cleavage by **5** (60 μM) in the absence of an external agent has been also studied as a function of time (0 – 60 minutes) under similar conditions. The amount of SC form is found to decrease and that of NC form to increase with increase in incubation time. Also, it is noted that 50% of DNA cleavage (**Figure 8**) is reached within 30 minutes and the rate of DNA cleavage reaches the maximum within 50 minutes and then remains constant. The addition of radical scavengers SOD and NaN_3 does not significantly reduce the efficiency of DNA cleavage (**Figure 9**).[51] Interestingly, the higher cleavage activity of **5** is retained when the reactions are performed under anaerobic conditions, revealing the non-involvement of activated oxygen species. However, the possibility of involvement of diffusible hydroxyl radicals in the cleavage is not completely ruled out, since DMSO decreases the cleavage ability of **5** (**Figure 9**). Thus the involvement of **5** in partial intercalation, supported by the strong hydrophobic interaction of anthracenyl moiety, and the alkyl side chains of the primary ligand, leads to stronger DNA-binding of the complex and higher distortions in DNA double helix, hence the higher order of DNA cleavage activity even in the absence of an activator.[52]

Cytotoxicity studies

MTT Assay

The cytotoxic activity of the present complexes against MCF-7 human breast cancer cell lines has been investigated in aqueous buffer solution in comparison with the widely used drug cisplatin under identical conditions by using MTT assay. The IC_{50} values (**Table 9**) obtained by plotting the cell viability against concentrations of the complexes reveal that all the complexes exhibit cytotoxicity higher than cisplatin for both 24 and 48 h incubations. The observed IC_{50} values at 48 h are lower than those at 24 h, revealing that the cell killing activity of the complexes is time dependent. Also, the cytotoxicity of the complexes follows the order **5** > **4** > **3** > **2** > **1**, which is consistent with the strong DNA binding and cleaving ability (in the absence of a reductant) of the complexes (cf. above). Interestingly, **5** exhibits cytotoxicity 15 times more potent than cisplatin for both 24 and 48 h incubation, and 1.5 – 3.0 times higher than the mixed ligand copper(II) complexes of tridentate ligand bba[12] and pmdt[13] with phen co-ligand, irrespective of the cell line used. Obviously, the partial intercalation of phen ring, supported by the hydrophobic interaction of appended anthracene and the alkane backbone and alkyl side

chain, is important. Thus **5** is proposed as a cytotoxic drug more potent than **1 - 4** and further studies are needed to confirm its potential as a cytotoxic agent.

AO/EB staining assay

The apoptotic morphologies induced by **1** – **5** have been investigated by using acridine orange/ethidium bromide (AO/EB) staining and adopting fluorescence microscopy (**Figure 10**). The cytological changes observed are classified into four types[17,31] according to the fluorescence emission and morphological features of chromatin condensation in the AO/EB stained nuclei: (i) viable cells having uniformly green fluorescing nuclei with highly organized structure; (ii) early apoptotic cells (which still have intact membranes but have started undergoing DNA fragmentation) having green fluorescing nuclei, but peri-nuclear chromatin condensation is visible as bright green patches or fragments; (iii) late apoptotic cells having orange to red fluorescing nuclei with condensed or fragmented chromatin; and (iv) necrotic cells, swollen to large sizes, having uniformly orange to red fluorescing nuclei with no indication of chromatin fragmentation. These morphological changes observed for **1 - 5** suggest that the cells are committed to more efficient apoptotic cell death.[53] The positively charged metal complexes are expected to adhere to the plasma membrane by electrostatic attraction before its transport across the membrane by the difference in concentration gradient of the complexes,[12,13,17] and eventually get released at various organelles in the cell to perform the cellular activities and then interfere with the cellular function of DNA leading to apoptosis. Similar observations have been made by us earlier for the mixed ligand complexes $[Cu(tdp)(3,4,7,8\text{-tmp})]^{+}$,[16] $[Cu(L\text{-tyr})(5,6\text{-dmp})]^{+}$ [15] and $[Cu_2(LH)_2(5,6\text{-dmp})_2(ClO_4)_2]^{2+}$.[14] Also, **4** and **5** cause more cells to preferentially take to one particular mode of cell death during 24 h treatment, and their higher apoptosis-inducing ability may originate from the partial intercalation of phen co-ligand, and the strong hydrophobic interaction of the anthracene moiety, modulated by the ethylene/propylene ligand backbone, and the alkyl side chain of primary ligands, which facilitates the permeation of the complexes across the cell membrane. As the apoptosis-inducing ability is critical in determining the efficacy of an anticancer drug, **4** and **5** with apoptosis inducing ability higher than the other complexes are predicted to function as more efficacious anticancer drugs. Further studies are needed in this direction to confirm the mode of cell death induced by the complexes.

Conclusions

A series of new mixed ligand copper(II) complexes of the type $[Cu(L)(phen)(ACN)]^{2+}$, where L is a simple bidentate Schiff base ligand (L1-L5) with appended anthracenyl moiety, has been isolated and characterized. The X-ray crystal structure of $[Cu(L5)(phen)(ACN)]^{2+}$ cation contains Cu(II) in a square pyramidal distorted trigonal bipyramidal coordinated geometry. The same complex exhibits DNA binding affinity higher than the other complexes due to partial intercalation of phen co-ligand, supported by the hydrophobic interaction of anthracenyl moiety, as tuned by the propylene ligand backbone, and the alkyl side chains of the primary ligand. Interestingly, the same complex completely degrades the supercoiled form of DNA without the requirement of an external agent even at 40 μM complex concentration, and exhibits cytotoxicity against MCF-7 human breast cancer cell line with potency higher than the widely used drug cisplatin. Further mechanistic and cellular uptake studies are essential to assess the anticancer activity of the novel non-covalently DNA binding and cleaving mixed ligand Cu(II) complex. The present study suggests that the aromatic ligand moieties like anthracene, benzimidazole etc, apart from the partially intercalating phen co-ligand, may be incorporated when a copper-based anticancer drug is designed.

Supplementary material

CCDC 927246 contains the supplementary crystallographic data for this paper. These data can be obtained free of charge from the Cambridge Crystallographic Data Centre via http://www.ccdc.cam.ac.uk/data_request/cif.

Acknowledgements

The present work is supported by DST Nano Mission [Scheme No. SR/NM/NS-110/2010(G)] and CSIR projects (CSIR/01(2462)/11/EMR-II). The X-ray diffraction facility was created by funding from Department of Science and Technology (DST-FIST), New Delhi and fluorescence spectral facilities were created by University Grants Commission (SAP), New Delhi in the Department of Chemistry, Bharathidasan University, Tiruchirappalli.

References

1. E. R. Jamieson and S. J. Lippard, *Chem. Rev*., 1999, **99**, 2467.

2. B. Rosenberg, L, Van Camp, J.E. Trosko and V.H. Mansour, *Nature* 1969, **222**, 385.

3. R. Huang, A. Wallqvist and D.G. Covell, *Biochem. Pharm.* 2005, **69**, 1009.

4. J. M. Rademaker-Lakhai, D. Van den Bongard, D. Pluim, J. H. Beijnen and J. H. Schellens, *Clin. Cancer Res.,* 2004, **10**, 3717.

5. J. D. Ranford, P.J. Sadler and D.A. Tocher, *J. Chem. Soc. Dalton Trans.,* 1993, 3393.

6. C. Marzano1, M. Pellei, F. Tisato and C. Santini, *Anti-Cancer Agents in Medicinal Chemistry* 2009, 9, 185.

7. I. Kostova, *Curr. Medi. Chem. Anticancer agents*, 2005, **5**, 591.

8. D. Desbouis, I. P. Troitsky, M. J. Belousoff, L. Spiccia and B. Graham, *Coord. Chem. Rev.,* 2012, **256**, 897.

9. J. He, P. Hu, Y.J. Wang, M.L. Tong, H. Sun, Z.W. Mao and L. N. Ji, *Dalton Trans.,* 2008, 3207.

10. L. J. Garcia-Gimenez, M. Gonzalez-Alvarez, M. Liu-Gonzalez, B. Macias, J. Borras and G. Alzuet, *J. Inorg. Biochem.,* 2009, **103**, 923.

11. P. Jaividhya, R. Dhivya, M.A. Akbarsha and M. Palaniandavar, *J. Inorg. Biochem.,* 2012, **114**, 94.

12. R. Loganathan, S. Ramakrishnan, E. Suresh, A. Riyasdeen, M.A. Akbarsha and M. Palaniandavar, *Inorg. Chem.,* 2012, **51**, 5512.

13. M. Ganeshpandian, R. Loganathan, S. Ramakrishnan, A. Riyasdeen, M. A. Akbarsha and M. Palaniandavar, *Polyhedron* 2012, **52**, 924-938**.**

14. S. Ramakrishnan, D. Shakthipriya, E. Suresh, V.S. Periasamy, M.A. Akbarsha and M. Palaniandavar, *Inorg. Chem*., 2011, **50**, 6458.

15. S. Ramakrishnan, V. Rajendiran, M. Palaniandavar, V.S. Periasamy, B. S Srinag, H. Krishnamurthy and M. A. Akbarsha, *Inorg. Chem.,* 2009, **48**, 1309–1322.

16. V. Rajendiran, R. Karthik, M. Palaniandavar, H.S. Evans, V.S. Periasamay, M.A. Akbarsha, B.S. Srinag and H. Krishnamurthy, *Inorg. Chem.,* 2007, **46**, 8208.

17. R. Loganathan, S. Ramakrishnan, E. Suresh, M. Palaniandavar, A. Riyasdeen, M.A. Akbarsha, *Dalton Trans.* 2014, **43**, 6177.

18. C. Rajarajeswari, R. Loganathan, E. Suresh, M. Palaniandavar, A. Riyasdeen and M.A. Akbarsha, *Dalton Trans.,* 2013, **42**, 8347.

19. C. Rajarajeswari, M. Ganeshpandian, M. Palaniandavar, A. Riyasdeen and M.A. Akbarsha, *J. Inorg. Biochem.,* 2014, **140**, 255.

20. (a) V. Rajendiran, M. Murali, E. Suresh, M. Palaniandavar, V. S. Periasamy and M. A. Akbarsha, *Dalton Trans.,* 2008, 2157-2170. (b) P. U. Maheswari and M. Palaniandavar, *Inorg. Chim. Acta*. 2004, **357**, 901. (c) P. U. Maheswari and M. Palaniandavar, *J. Inorg. Biochem*. 2004, **98**, 219.

21. S. Ramakrishnan, E. Suresh, A. Riyasdeen, M.A. Akbarsha and M. Palaniandavar, *Dalton Trans.,* 2011, **40**, 3245.

22. S. Ramakrishnan, E. Suresh, A. Riyasdeen, M.A. Akbarsha and M. Palaniandavar, *Dalton Trans*, 2011, **40**, 3524.

23. M. Ganeshpandian, S. Ramakrishnan, M. Palaniandavar, A. Riyasdeen, and M. A. Akbarsha, *J. Inorg. Biochem.,* 2014, **140**, 202-212**.**

24. M. Inclán, M.T. Albelda, J.C. Frías, S. Blasco, B. Verdejo, C. Serena, C. Salat-Canela, M.L. Díaz, A. García-España and E. García-España *J. Am. Chem. Soc.,* 2012, **134**, 9644.

25. (a) S. K. Carter, D. Rall, P. Schein, R. D. Davis, H. B. Wood, Jr., R. Engle, J. P. Davignon, J. M. Venditti, S. A. Schepartz, B. R. Murray and C. G. Zubrod. 1968. Pseudourea *NSC 56054 Clinica Brochure*. National Cancer Chemotherapy Institute, p. 2. (b) R.K.Y. Zee-Cheng and C.C. Cheng, *J. Med. Chem.,* 1978, **21**, 291.

26. L. Fabbrizzi, M. Licchelli, A. Perrotti, A. Poggi, G. Rabaioli and A. Taglietti*, J. Chem. Soc., Perkin Trans.,* 2001, **2**, 2108

27. S.A. McFarland and F.S. Nathaniel, *J. Am. Chem. Soc.*, 2001, **123**, 1260.

28. C. Santini, M. Pellei, V. Gandin, M. Porchia, F. Tisato and C. Marzano, *Chem. Rev.,* 2014, **114**, 815−862.

29. N. Aliaga-Alcalde, P. Marques-Gallego, M. Kraaijkamp, C. Herranz-Lancho, H. Dulk, H. Gorner, O. Roubeau, S.J. Teat, T. Weyhermuller and J. Reedijk, *Inorg. Chem.,* 2010, **49** 9655.

30. (a) X. Q. Cai, N. Pan and G. Zou, *BioMetals* 2007, 20, 1. (b) P. U. Maheswari, M. vander Ster, S. Smulders, S. Barends, G. P. van Wezel, C. Massera, S. Roy, H. den Dulk, P. Gamez and J. Reedijk, *Inorg. Chem.,* 2008, **47**, 3719. (c) D. Chen, V. Milacic, M. Frezza and Q. P.

Dou, *Curr. Pharm. Des.,* 2009, 15, 777. (d) S. Tardito and L. Marchio, *Curr. Med. Chem.,* 2009, **16**, 1325.

31. M. Ganeshpandian, R. Loganathan, E. Suresh, A. Riyasdeen, M. A. Akbarsha and M. Palaniandavar, *Dalton Trans.,* 2014, **43**, 1203.

32. D.D. Perrin, W.L.F. Armarego, D.R. Perrin, *Purification of Laboratory Chemicals*, Pergamon Press, Oxford, 1980.

33. S. Dhar, D. Senapati, P.K. Das, P. Chattopadhyay, M. Nethaji and A.R. Chakravarty, *J. Am. Chem. Soc.,* 2003, **125**, 12118.

34. J. Marmur, *J. Mol. Biol.*, 1961, **3**, 208.

35. SMART & SAINT Software Reference manuals, version 5.0; Bruker AXS Inc., Madison, WI, 1998.

36. SHELXTL Reference Manual, version 5.1; Bruker AXS Inc., Madison, WI, 1998

37. J.D. McGhee and P.H von Hippel, *J. Mol. Biol.,*1974, **86**, 469.

38. J. Bernadou, G. Pratviel, F. Bennis, M. Girardet and B. Meunier, *Biochemistry*, 1989, **28**, 7268-7275.

39. M. Blagosklonny and W.S. El-Diery, *Int. J. Cancer,* 1996, **67**, 386.

40. M. R. Duff Jr., V. K. Mudhivarthi and C. V. Kumar, *J. Phys. Chem. B,* 2009, 113, 1710.

41. M. Palaniandavar, I. Somasundaram, M. Lakshminarayanan and H. Manohar, *Dalton Trans.,* 1996, 1333.

42. J. E. Huheey, E. A.Keiter,; R. L. Keiter and O. K. Medhi, *Inorganic Chemistry, Principles of Structure and Reactivity*; Pearson Education: Upper Saddle River, NJ, 2006, 425.

43. G. Murphy, C. Murphy, B. Murphy and J. Hathaway, *J. Chem. Soc., Dalton Trans.,* 1997, 2653.

44. P. Nagle, E. O'Sullivan and B.J. Hathaway, *J. Chem. Soc., Dalton Trans.,* 1990, 3399.

45. A.W. Addison, T.N. Rao, J. Reedijk, J. Van Rijn and G. C. Verschoor, *J. Chem. Soc., Dalton Trans.* 1984, 1349.

46. S.A. Tysoe, R.J. Morgan, A.D. Baker and T.C. Strekas, *J. Phys. Chem.,* 1993, **97**, 1707.

47. A. Wolfe, G.H. Shimer and T. Meehan, *Biochemistry*, 1987, **26**, 6392.

48. D. L. Boger, S. R. Fink, S. R. Brunette, W. C. Tse and M. P. Hedrick, *J. Am. Chem. Soc,*. 2001, **123**, 5878.

49. B. Selvakumar, V. Rajendiran, P.U. Maheswari, H.S. Evans and M. Palaniandavar, *J. Inorg. Biochem.,* 2006, **100**, 316.

50. S. Ramakrishnan and M. Palaniandavar, *J. Chem. Sci.,* 2005, **117**, 179.

51. Q. Liang, D. C. Arianias and E. C. Long, *J. Am. Chem. Soc*., 1998, **120**, 248.

52. E. Lamour, S. Routier, J. L. Bernier, J. P. Catteau, C. Bailly and H. Vezin, *J. Am. Chem. Soc.,* 1999, **121**, 1862.

53. I. M. Ghobrial, T.E. Witzig and A. A. Adjei*, Cancer J. Clin.,* 2005, **55**, 178.

Table 1. Crystal data and structure refinement for $[Cu(L5)(phen)(ACN)](ClO_4)_2$ **5**

	$[Cu(L5)(phen)(ACN)](ClO_4)_2$
Empirical formula	$C_{33}H_{31}Cl_2CuN_5O_8$
Formula weight	760.07
Crystal system	Monoclinic
Space group	P21/n
Crystal size	0.44 x 0.31 x 0.23 mm
Temperature (K)	100
λ, Å (Mo K_α)	0.71073
a, Å	11.362(6)
b, Å	23.930(12)
c, Å	12.192(6)
β°	108.863(9)
Z	4
Density (calculated), Mg/m^3	1.607
θ for data collection	1.7, 25.0
Refinement method	Full-matrix least-squares on F^2
Unique reflections [$R_{(int)}$]	26976/7588 [R (int) = 0.028]
F (000)	445
Final R indices [I>2 σ(I)]	
[a]R1	0.1014
[b]wR2	0.2492
[c]S	1.091
Largest difference in peak and hole, e $Å^{-3}$	-0.58, 0.77

[a]$R1 = [\Sigma(||Fo|-|Fc||)/\Sigma|Fo|]$ [b]$wR2 = \{[\Sigma(w(Fo^2-Fc^2)^2)/\Sigma(wFo^4)]^{1/2}\}$

[c]Goodness-of-fit on F^2

Table 2. Selected bond distances (Å) and angles (°) for complex **5**

Bond distance		**Bond angle**	
Cu1-N1	1.996(6)	N1-Cu1-N2	81.1(2)
Cu1-N2	2.096(6)	N1-Cu1-N3	176.0(3)
Cu1-N3	2.010(6)	N1-Cu1-N4	91.3(2)
Cu1-N4	2.043(6)	N1-Cu1-N5	86.6(2)
Cu1-N5	2.201(6)	N2-Cu1-N3	99.7(2)
		N2-Cu1-N4	130.3(2)
		N2-Cu1-N5	122.4(2)
		N3-Cu1-N4	91.2(2)
		N3-Cu1-N5	89.7(2)
		N4-Cu1-N5	105.8(2)

Table 3. Electronic[a] spectral properties of Cu(II) complexes

Complex		λ_{max} in nm (ε, M^{-1} cm^{-1})		
		Ligand field[b]	Ligand based[c]	Intraligand transition
$[Cu(L1)(phen)(ACN)](ClO_4)_2$	**1**	705 (98)	253 (105300)	353 (730), 371 (1340), 384 (860)
$[Cu(L2)(phen)(ACN)](ClO_4)_2$	**2**	600 (70)	258 (114200)	359 (780), 377 (1220), 391 (890)
$[Cu(L3)(phen)(ACN)](ClO_4)_2$	**3**	647 (110)	256 (120900)	350 (840), 369 (1370), 386 (940)
$[Cu(L4)(phen)(ACN)](ClO_4)_2$	**4**	620 (130)	265 (93000)	353 (1790), 372 (4190), 387 (2520)
$[Cu(L5)(phen)(ACN)](ClO_4)_2$	**5**	695 (150)	256 (112900)	349 (1510), 368 (4190), 379 (2700)

[a]In ACN solution, [b]Concentration, 5×10^{-3} M, [c]Concentration, 1×10^{-5} M

Table 4. Ligand based absorption spectral properties of Cu(II) complexes bound[a] to calf thymus DNA.

Complex		Ligand-based					
		λ_{max} (nm)	R	Change in absorbance	Δε (%)	Red shift (nm)	$K_b \times 10^5$ (M^{-1})
$[Cu(L1)(phen)(ACN)](ClO_4)_2$	**1**	253	25	Hypochromism	20	2	0.9 ± 0.2
$[Cu(L2)(phen)(ACN)](ClO_4)_2$	**2**	258	25	Hypochromism	25	3	1.1 ± 0.3
$[Cu(L3)(phen)(ACN)](ClO_4)_2$	**3**	256	25	Hypochromism	31	2	1.2 ± 0.1
$[Cu(L4)(phen)(ACN)](ClO_4)_2$	**4**	265	25	Hypochromism	33	2	1.6 ± 0.6
$[Cu(L5)(phen)(ACN)](ClO_4)_2$	**5**	256	25	Hypochromism	46	4	2.3 ± 0.3

[a] Measurements were made at R=25, where R = [DNA]/[Complex], concentration of solution of copper(II) complex = 1×10^{-5} M

Table 5. Luminescence properties of the copper(II) complexes in the absence and presence of CT DNA

Complexes		$^{a}\lambda_{ex}$ (nm)	$^{b}\lambda_{em}$ (nm)	K_b' (M) × 10^5	n
$[Cu(L1)(phen)(ACN)](ClO_4)_2$	**1**	380	520	0.6 ± 0.05	3.0
$[Cu(L2)(phen)(ACN)](ClO_4)_2$	**2**	383	525	4.0 ± 0.02	4.2
$[Cu(L3)(phen)(ACN)](ClO_4)_2$	**3**	382	524	6.0 ± 0.03	4.7
$[Cu(L4)(phen)(ACN)](ClO_4)_2$	**4**	381	521	9.0 ±0.06	4.9
$[Cu(L5)(phen)(ACN)](ClO_4)_2$	**5**	385	525	13.0 ± 0.01	7.2

[a]Excitation wavelength maximum of the complexes; [b]Emission wavelength maximum of the complexes in the presence and absence of CT DNA; Measurements were made at R = 0 – 10, where R = [DNA]/[complex], concentration of copper complex solutions = 1×10^{-5} M.

Table 6. Cleavage of SC pUC19 DNA (40 μM) by complexes **1** – **5** (100 μM) in the absence of an external agent in a buffer containing 5 mM Tris HCl/50 mM NaCl (pH 7.1) at 37 ^{o}C

Lanes	Reaction conditions	Form (%)	
		SC	NC
1	DNA control	97.5	2.5
2	DNA + **1**	29.1	70.9
3	DNA + **2**	23.9	76.1
4	DNA + **3**	22.5	77.5
5	DNA + **4**	3.9	96.1
6	DNA + **5**	0.8	99.2

Table 7. Concentration-dependent cleavage data of SC pUC19 DNA (40 μM) by complex **4** in the absence of an activator in a buffer containing 5 mM Tris HCl/50 mM NaCl (pH 7.1) at 37 ^{o}C.

Lanes	Reaction conditions	Form (%)	
		SC	NC
1	DNA control	98.8	1.2
2	DNA + **4** (10 μM)	39.5	40.5
3	DNA + **4** (20 μM)	54.1	45.9
4	DNA + **4** (40 μM)	37.6	62.4
5	DNA + **4** (60 μM)	13.9	86.1
6	DNA + **4** (80 μM)	10.6	89.4
7	DNA + **4** (100 μM)	4.3	95.7

Table 8. Concentration-dependent cleavage data of SC pUC19 DNA (40 μM) by complex **5** in the absence of an activator in a buffer containing 5 mM Tris HCl/50 mM NaCl (pH 7.1) at 37 ^{o}C.

Lanes	Reaction conditions	Form (%)	
		SC	NC
1	DNA control	98.1	1.9
2	DNA + **5** (10 μM)	72.0	28.0
3	DNA + **5** (20 μM)	47.6	52.4
4	DNA + **5** (40 μM)	12.3	87.7
5	DNA + **5** (60 μM)	5.6	94.4
6	DNA + **5** (80 μM)	0.9	99.1
7	DNA + **5** (100 μM)	0.4	99.6

Table 9. *In vitro* cytotoxicity assay for complexes **1 - 5** against MCF-7 human breast cancer cell line (IC_{50} values are in μM)

Complex	[a]IC_{50}, μM	
	24 h	48 h
$[Cu(L1)(phen)(ACN)](ClO_4)_2$ **1**	13.0 ± 0.3	7.9 ± 0.5
$[Cu(L2)(phen)(ACN)](ClO_4)_2$ **2**	9.2 ± 0.1	4.8 ± 0.2
$[Cu(L3)(phen)(ACN)](ClO_4)_2$ **3**	6.1 ± 0.1	2.2 ± 0.1
$[Cu(L4)(phen)(ACN)](ClO_4)_2$ **4**	5.9 ± 0.4	2.4 ± 0.5
$[Cu(L5)(phen)(ACN)](ClO_4)_2$ **5**	2.5 ± 0.1	1.2 ± 0.1
cisplatin	36.5 ± 0.1	18.7± 0.1
phen	200.0 ± 7.1	183.7± 9.5

[a]IC_{50} = concentration of drug required to inhibit growth of 50% of the cancer cells (in μM)

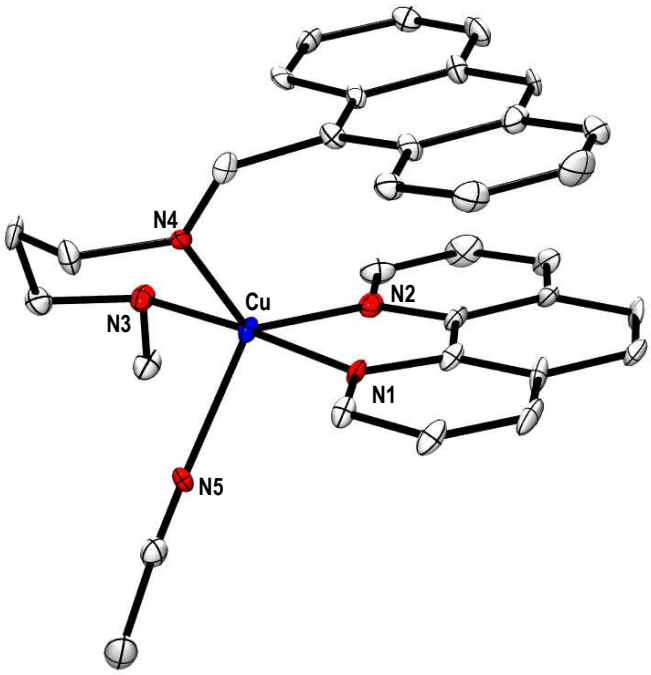

Figure 1. ORTEP representation of the complex cation $[Cu(L5)(phen)(ACN)]^{2+}$ of **5** showing the atom numbering scheme. All the hydrogen atoms and percholrate counter ion are omitted for clarity.

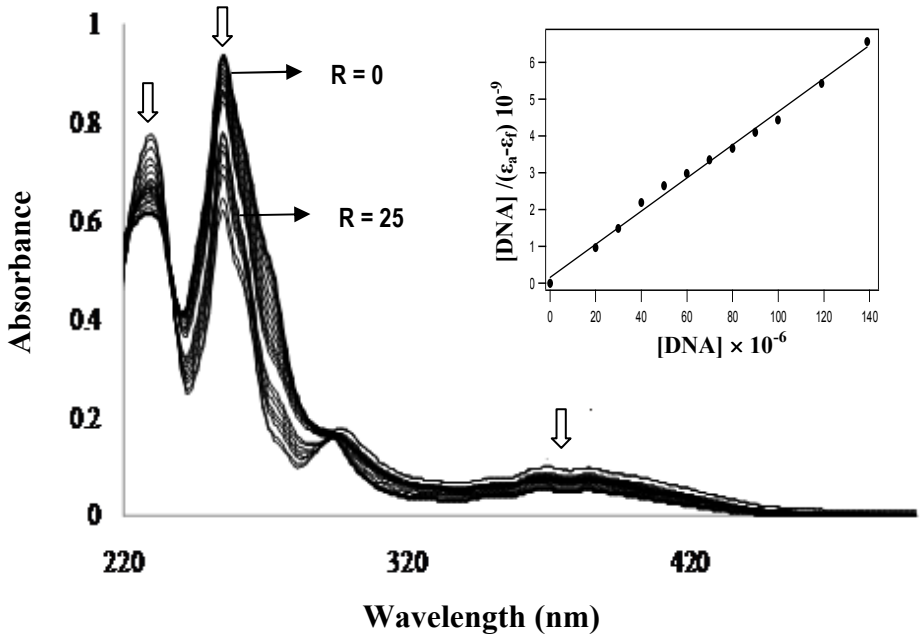

Figure 2. Absorption spectra of $[Cu(L5)(phen)(ACN)]^{2+}$ (1×10^{-5} M) in 5 mM Tris HCl buffer at pH 7.1, in the absence ($R = 0$) and presence ($R = 25$) of increasing amounts of DNA. Inset: Plot of $[DNA]/(\varepsilon_a - \varepsilon_f)$ *vs* [DNA] for $[Cu(L5)(phen)(ACN)]^{2+}$.

(A) (B)

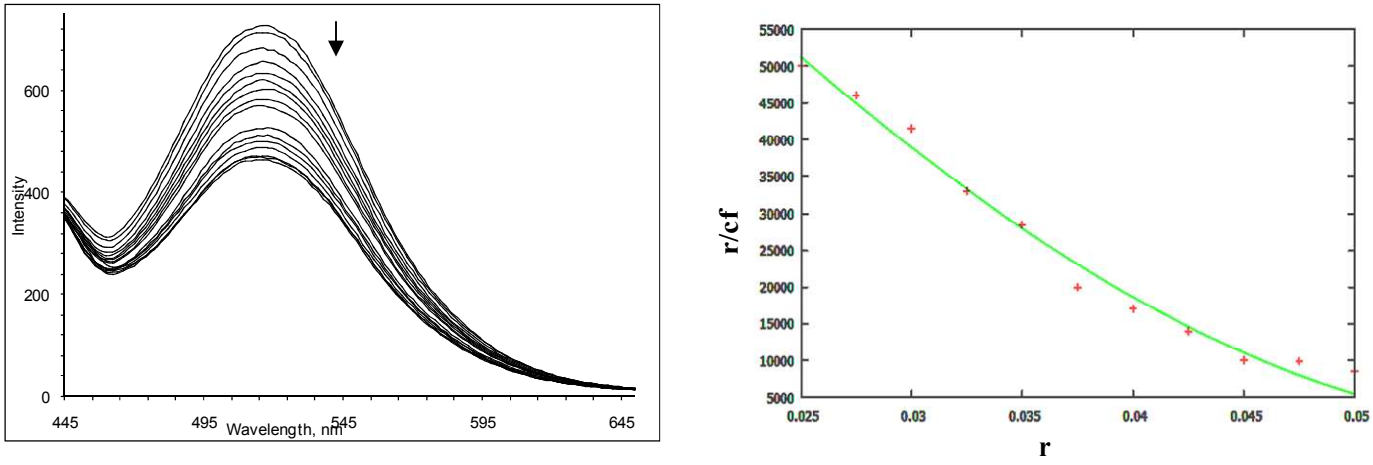

Figure 3. (A) Emission spectra of $[Cu(L5)(phen)(ACN)]^{2+}$ (1×10^{-5} M) in **5** mM Tris HCl buffer at pH 7.1, in the absence ($R = 0$) and presence ($R = 10$) of increasing amounts of DNA. (B) Plot of r/c_f vs r for $[Cu(L5)(phen)(ACN)]^{2+}$. The best fit line, superimposed on the data, according to McGhee and von Hippel equation (2) yields K_b'

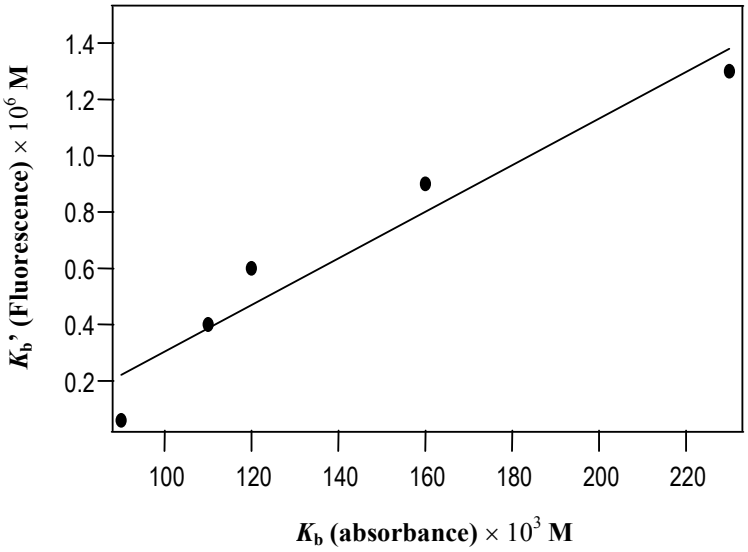

Figure 4. Plot of K_b (UV-Vis) vs K_b' (Fluorescence) for $[Cu(L1\text{-}L5)(phen)(ACN)]^{2+}$

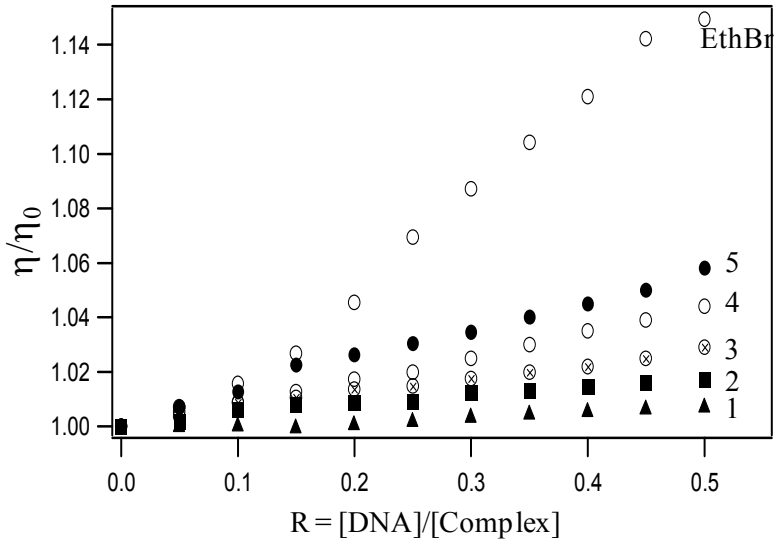

Figure 5. The effect of $[Cu(L1)(phen)(ACN)](ClO_4)_2$ (**1**), $[Cu(L2)(phen)(ACN)](ClO_4)_2$ (**2**), $[Cu(L3)(phen)(ACN)](ClO_4)_2$ (**3**), $[Cu(L4)(phen)(ACN)](ClO_4)_2$ (**4**), $[Cu(L5)(phen)(ACN)](ClO_4)_2$ (**5**) and on the viscosity of CT DNA; relative specific viscosity (η/η_0) vs. 1/R.

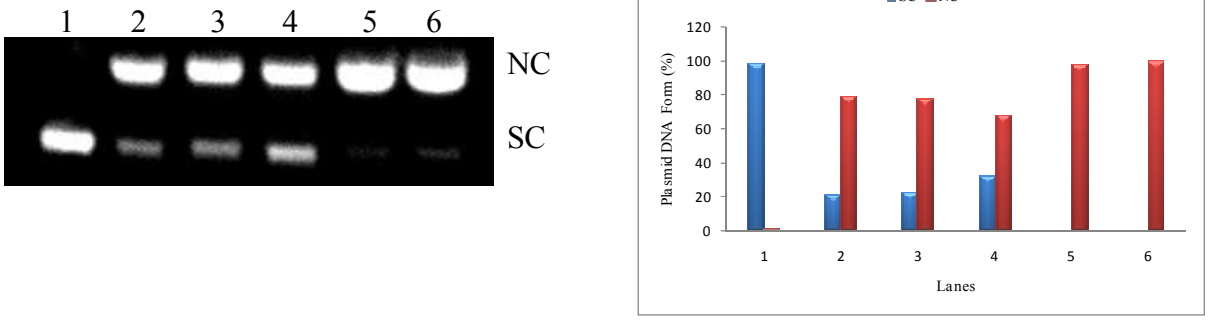

Figure 6. (A) Gel electrophoresis diagram showing the cleavage of supercoiled pUC19 DNA (40 μM) by complexes **1** - **5** (100 μM) in 5 mM Tris-HCl/50 mM NaCl buffer at pH 7.1 and 37 °C with an incubation time of 1 hr in absence of an external agent: lane 1, DNA; lane 2, DNA + complex **1**; lane 3, DNA + complex **2**; lane 4, DNA + complex **3**; lane 5, DNA + complex **4**; lane 6, DNA + complex **5**; Forms SC and NC are supercoiled and nicked circular DNA, respectively. (B) Relative amounts of the different DNA forms in presence of **1** – **5**.

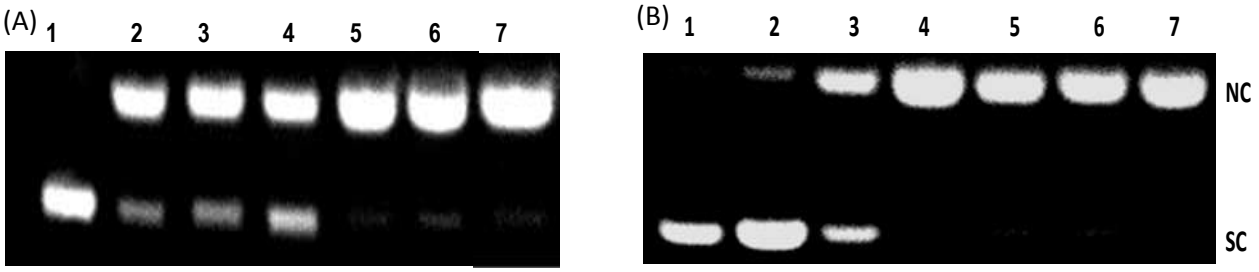

Figure 7. (A) Concentration dependent DNA (40 μM) cleavage by $[Cu(L4)(phen)(ACN)](ClO_4)_2$ **4**/$[Cu(L5)(phen)(ACN)](ClO_4)_2$ **5** (10-100 μM) in 5 mM Tris-HCl–50 mM NaCl at pH = 7.1 at 37 ^oC for 1 hr. (A) lane 1, DNA; lane 2, DNA + **4** (10 μM); lane 3, DNA + **4** (20 μM); lane 4, DNA + **4** (40 μM); lane 5, DNA + **4** (60 μM); lane 6, DNA + **4** (80 μM); lane 7, DNA + **4** (100 μM). (B) lane 1, DNA; lane 2, DNA + **5** (10 μM); lane 3, DNA + **5** (20 μM); lane 4, DNA + **5** (40 μM); lane 5, DNA + **5** (60 μM); lane 6, DNA + **5** (80 μM); lane 7, DNA + **5** (100 μM). SC and NC are supercoiled and nicked circular forms of DNA, respectively.

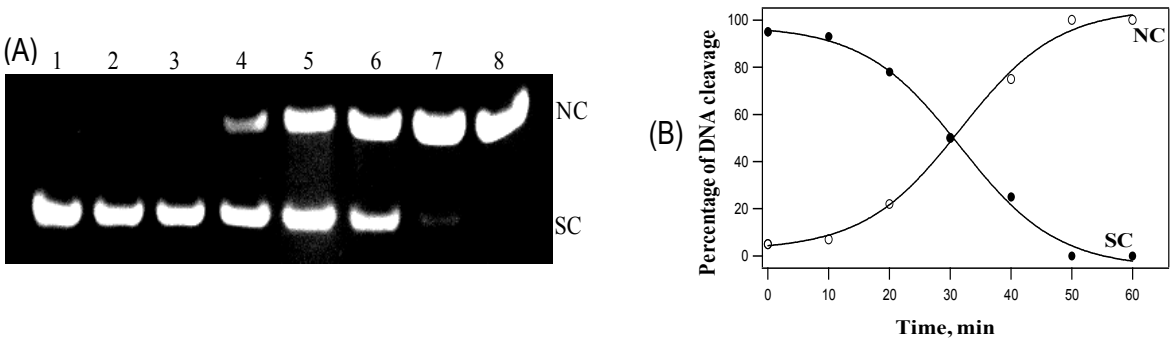

Figure 8. (A) Time course of supercoiled pUC19 DNA (40 μM) cleavage by complex **5** (60 μM) in a 5 mM Tris-HCl/50 mM NaCl buffer at pH 7.1 and 37 °C with incubation times of 0, 10, 20, 30, 40, 50, and 60 min for lanes 2-8. (B) Plot of cleavage of supercoiled pUC19 DNA showing the decrease in form I (SC DNA) and the formation of form II (NC DNA) with an incubation time using 60 μM concentration of **5**.

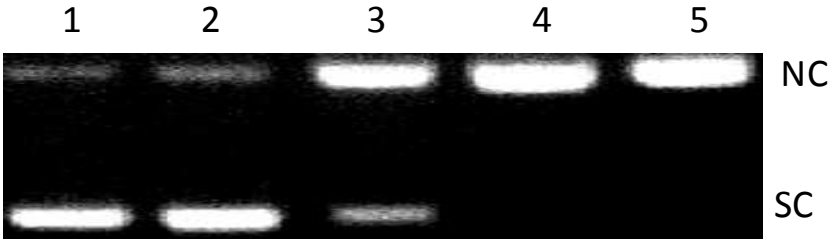

Figure 9. Mechanistic investigation of cleavage of **5** without any activator in a 5 mM Tris-HCl/50 mM NaCl buffer at pH 7.1 and 37 °C with an incubation time of 1 hr; lane 1, DNA; lane 2, DNA + DMSO + complex **5**; lane 3, DNA + SOD + complex **5**; lane 4, DNA + NaN_3 + complex **5**; lane 5, DNA + Argon + complex **5**.

(A)

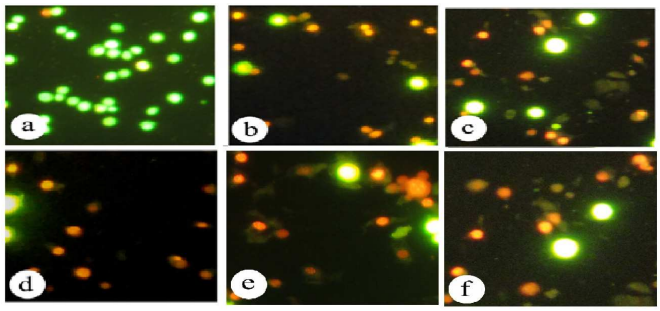

(B)

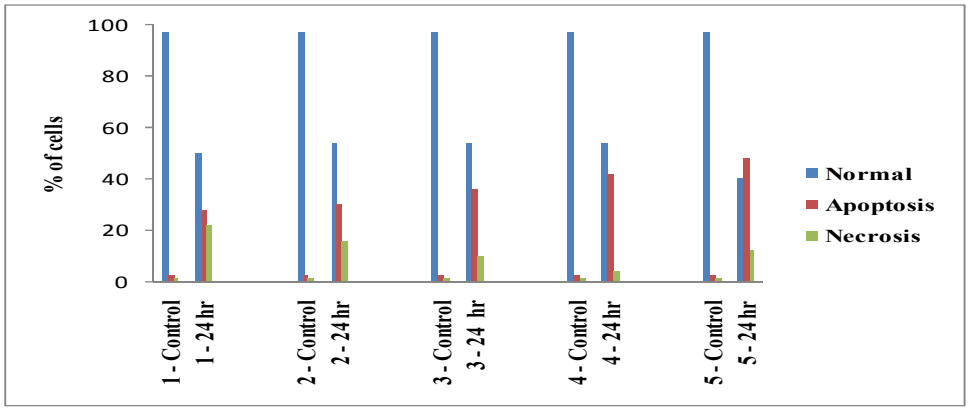

Figure 10. (A) AO/EB staining of MCF-7 human breast cancer cells. (a) Untreated cells, (b) treated with complex **1**, (c) complex **2**, (d) complex **3**, (e) complex **4** and (f) complex **5** with MCF-7 cells at 24 h of incubation, respectively (B) Graph shows manual count of apoptotic and necrotic cells in percentage. (Data are mean % ± SD% of each triplicate).

Colour Graphic

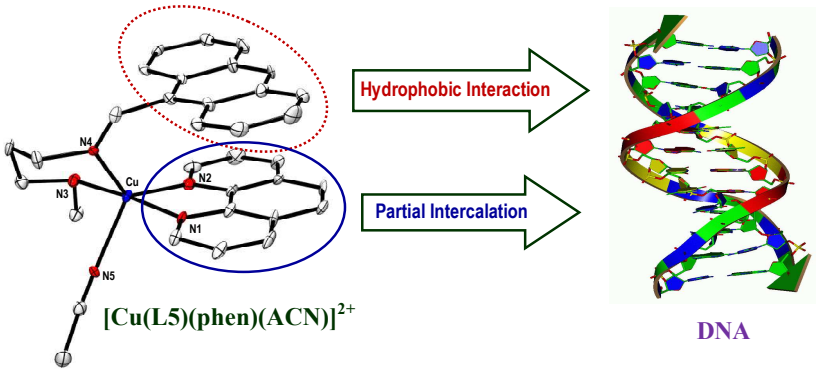

Text

While phen of $[Cu(L1\text{-}L5)(phen)(ACN)]^{2+}$ partially inserts into DNA base pairs the anthracenyl moiety of L1-L5 interacts with DNA hydrophobically.